IOP PUBLISHING JOURNAL OF PHYSICS D: APPLIED PHYSICS

J. Phys. D: Appl. Phys. **40** (2007) 4234–4240 doi:10.1088/0022-3727/40/14/019

The effect of annealing and ZnO dopant on the optoelectronic properties of ITO thin films

H A Mohamed

Physics Department, Faculty of Science, Sohag University, 82524 Sohag, Egypt

E-mail: hussein_abdelhafez2000@yahoo.com

Received 4 March 2007, in final form 4 May 2007
Published 29 June 2007
Online at stacks.iop.org/JPhysD/40/4234

Abstract

Thin films of indium tin oxide doped with ZnO thin films have been prepared by the electron-beam evaporation technique. The effects of heat treatment and ZnO content on the structural, optical and electrical properties of these films have been investigated. The optical transmission was found to improve with increasing ZnO ratio and annealing temperature. Enhancement of the film crystallinity or the grain size growth seemed to be associated with an improvement of the mobility carriers and hence the film conductivity. Transmittance values of 84–90% in the visible region and low electrical resistivity of 1.2×10^{-4}–1.3×10^{-4} Ω cm have been achieved for $(ITO)_{1-x}(ZnO)_x$ film with $x = 0.2$ annealed at temperature of 325 °C for 90 min and 120 min, respectively. Other optical parameters, namely optical energy gap, free carrier concentration, refractive index and extinction coefficient were studied.

1. Introduction

Indium tin oxide (ITO) films are considered as a promising transparent-conductive material. Therefore they are used in several optoelectronic devices, such as flat panel display [1,2], photovoltaic solar cells [3, 4], liquid crystal display [5, 6], biological devices [7] and heat reflection mirrors [8]. ITO is a degenerate n-type semiconductor with a wide band gap (3.5–4.3 eV), where the Fermi level is located above the conduction level [9]. Therefore, it possesses low resistivity and high transmission for visible and near-IR regions of the electromagnetic spectrum.

The degeneracy of ITO may be caused due to the high concentration of free carriers, that could be generated by Sn atom substitution of In atom giving out one extra electron and oxygen vacancies acting as two donors [10]. However, these highly concentrated free carriers lead to a degradation of the optical properties because of the increase in the reflectivity and free carrier absorption of light leading to an inhibition of the optical transmission of a film [11]. The solution to this problem may be attained by a compromise between electrical and optical properties; a mater could be achieved by improving the film ordering and reducing the scattering of the electrons [10]. ZnO has been actively investigated as an alternative material to ITO because ZnO is a non-toxic, inexpensive and abundant material. It is also chemically stable under hydrogen plasma processes that are commonly used for the production of solar cells [12]. Therefore, ZnO materials have been employed in various optoelectronic devices owing to their excellent photoelectric, thermal stable and optical properties.

It is reported that [13], the microstructure nature of ZnO is an advantage in inducing an increase in ITO films grain size, reducing electron scattering and improving electrical conduction. Minami *et al* [14] have prepared transparent and conductive (ITO/Zn) thin films by the magnetron sputtering system. The obtained results were found to be considerably affected by the Zn content and the preparation conditions. On the other hand, Liu *et al* [15] have described transparent and conductive films cosputtered with ITO and ZnO targets using an rf magnetron cosputtering system, to maintain the superior electrical properties and extend the additional applications of the electrical and optical properties in associated optoelectronic devices. It was found that ITO films doped with ZnO have a low resistivity value and a sufficient optical transmittance at visible wavelengths compared with undoped ITO. Recently [16], the effect of substrate temperature on the electrical and optical properties of ITO : ZnO films was studied. It was noted that the optical and

electrical properties of zinc oxide doped indium tin oxide films are strongly dependent on the preparation conditions, substrate temperature and ZnO ratio.

In this work, the effect of ZnO as a dopant and the heat treatment on the structural, optical and electrical properties of ITO thin films prepared by the electron beam evaporation technique has been studied. The electron beam evaporation technique, which provides an economical and efficient use of evaporant, was used to prepare ITO : ZnO thin films from bulk tablets prepared by a sintering process, which helped to produce lumps of powder material in bulky form without affecting their chemical properties, while their physical properties approach those of single phase [17]. A compromise between low resistivity and high transmission of light has been made in order to examine the quality of films as transparent-conductive ones.

2. Experimental details

SnO_2, In_2O_3 and ZnO powders (Aldrich Chemical Co.) with 99.999% purity and mean particle size of $\sim$0.46 μm were ground separately and sieved. Appropriate ratios of In_2O_3 (90 wt%) and SnO_2 (10 wt%) were used to prepare ITO powder. A mixture of $(ITO)_{1-x}(ZnO)_x$ thin films with $x = 0.05$, 0.1, 0.15, 0.2 and 0.25 was prepared. To increase complete mixing, the mixtures were ground for at least three hours. Then, they were made into tablet form using a cold pressing technique. Sintering was performed for the present mixtures at 900 °C for 4 h.

An Edwards high vacuum coating unit model E306A under pressure of 5×10^{-5} and 2×10^{-5} Torr before and during film deposition was used to prepare $(ITO)_{1-x}(ZnO)_x$ thin films onto ultrasonically cleaned microscope glass slides. The film thickness (150 nm) and deposition rate were controlled by means of a digital film thickness monitor model TM200 Maxtek.

Structural analysis of as-deposited and annealed films was carried out on a Phillips PW-1710 Cu-k_α diffractometer ($\lambda = 1.541\,838$ Å) by varying the diffraction angle 2θ from 4 to 80 by a step width of 0.04 in order to evaluate the crystalline phase and crystallite orientation. The optical transmittance (T) and reflectance (R) in the wavelength range from 200 to 2500 nm at normal incidence were measured using a Jasco V-570 UV-VIS-NIR spectrophotometer.

The annealing temperature from 200 to 450 °C for 15 min and the annealing time from 5 to 120 min at a fixed temperature of 325 °C of the deposited films were carried out in a fully controlled furnace in air.

The electrical resistivity measurements were carried out using a Keithley 614 electrometer with simple two-probe contacts. The measurements were performed at room temperature. Electrical contacts were made by applying silver paste over the surface of the films with a separation of 2 mm. The mobility carriers (μ) were estimated using the relation $\mu = 1/N\,\rho\,e$, where N is the optical free carrier concentration, ρ is the measured electrical resistivity and e the electronic charge.

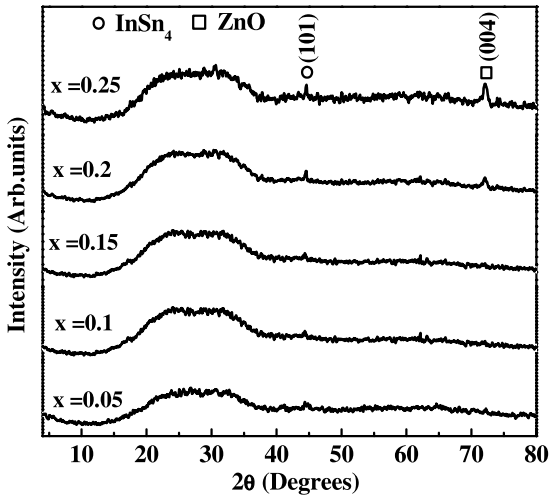

Figure 1. The x-ray diffraction of as-deposited $(ITO)_{1-x}(ZnO)_x$ films with different ratios of ZnO.

3. Results and discussion

3.1. Film structure

The x-ray diffraction patterns of as-deposited film $(ITO)_{1-x}(ZnO)_x$ with different ratios of zinc oxide are plotted in figure 1. All as-deposited films exhibit amorphous structure. For higher ZnO ratios, the peaks (0 0 4) and (1 0 1) corresponding to ZnO and InSn4, respectively, become more apparent. In addition, the (2 2 2) peak of ITO is observed for films annealed at 200 °C as shown in figure 2(*a*). Annealed films $(ITO)_{1-x}(ZnO)_x$ with $x = 0.2$ at 325 °C for 15 min were found to be associated with amorphous–polycrystalline transformation as shown in figure 2(*b*). The diffraction peaks (2 2 2), (4 0 0) and (4 4 1) indicate the formation of ITO. Three small diffraction peaks associated with the (1 0 1), (6 2 2) and (0 0 4) planes corresponding to InSn4, In2O3 and ZnO, respectively also appeared. Prolongation of the annealing period (t_{ann}) to 60 min for the $(ITO)_{1-x}(ZnO)_x$ film with $x = 0.2$ seemed to improve the film crystallinity, since the intensity of the observed peaks was relatively increased. In general, the ITO peak (2 2 2) has the highest value of intensity compared with the intensities of other peaks, indicating a favoured orientation towards the (2 2 2) crystallographic plane. Using the peak (2 2 2) corresponding to ITO the grain size was estimated from Scherrer equation [18] and plotted as a function of zinc oxide ratio in figure 3. It is clear that the grain size of $(ITO)_{1-x}(ZnO)_x$ films increases with increasing ratio x and reaches its highest value 36.17 nm at $x = 0.15$. With a further increase in the x ratio a slight decrease in grain size is observed.

3.2. Optical and electrical properties of as-deposited films

Figure 4(*a*) shows the optical transmittance (T%) of $(ITO)_{1-x}(ZnO)_x$ films for different concentrations of zinc oxide ratio (x) in the wavelength range from 200 to 2500 nm. The optical transmittance increased slightly with increasing ZnO ratio up to $x = 0.25$. The low values of transmittance may be due to oxygen deficiency resulting during the electron-beam evaporation process [19, 20]. This concept may be confirmed

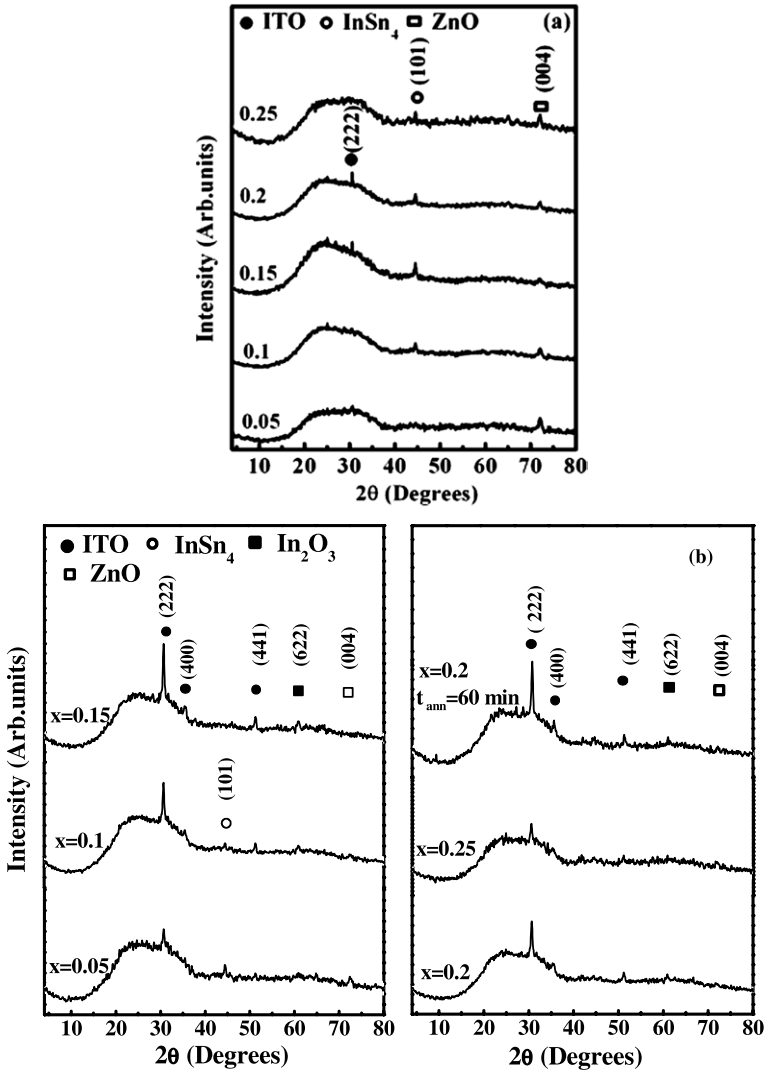

Figure 2. The x-ray diffraction of $(ITO)_{1-x}(ZnO)_x$ with $x = 0.05, 0.1, 0.15, 0.2$ and 0.25 annealed at 200 °C for 15 min (*a*) and at temperature 325 °C for 15 min, and the film with $x = 0.2$ annealed at 325 °C for 60 min (*b*).

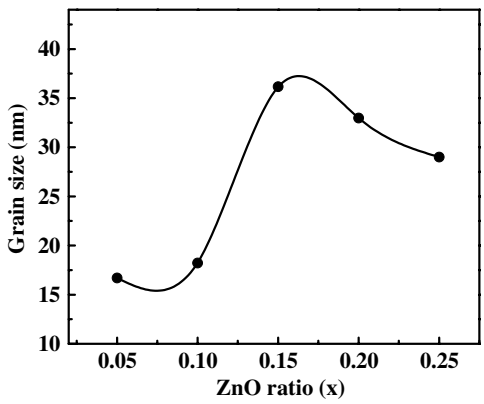

Figure 3. Variation of the grain size (nm) as a function of ZnO ratio for $(ITO)_{1-x}$ $(ZnO)_x$ films annealed at 325 °C for 15 min.

regarding the appearance of the InSn4 (1 0 1) peak on the x-ray diffraction patterns that emphasize the oxygen deficiency in the films. In addition, it is seen that the absorption edge is shifted to higher energy with increasing ZnO content, indicating an increase in the optical energy gap.

Figure 4(*b*) represents the reflectance ($R\%$) against the wavelength for different ratios of ZnO. The reflectance increases with increasing x ratio and attains its maximum value 50.6% for $x = 0.15$ in the NIR region. With a further increase in the x ratio, the reflectance starts to decrease. The optical parameters, namely free carrier concentration (N), refractive index (n) and extinction coefficient (k) were calculated as follows:

The real (n) and imaginary (k) parts of the refractive index have been determined from the transmission measurements using the following equation [21]:

$$n = \frac{1+R}{1-R} \pm \left[\left(\frac{R+1}{R-1} \right)^2 - (1+k^2) \right]^{1/2}, \qquad (1)$$

where $k = \alpha\lambda/4\pi$; α is the absorption coefficient. The absorption coefficient α of the films was determined directly from the spectrophotometer readings using the following equation [16]:

$$\alpha = \frac{2.303}{d} \log_{10} \left(\frac{1-R}{T} \right), \qquad (2)$$

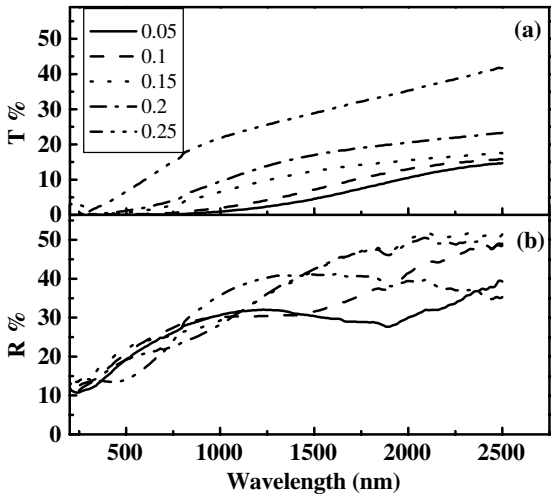

Figure 4. Transmittance (*a*) and reflectance (*b*) spectra of as-deposited $(ITO)_{1-x}(ZnO)_x$ films with different x ratios as a function of wavelength.

Table 1. Variations of the average refractive index (n), the average extinction coefficient (k) in the visible region, free carrier concentration (N) and electrical resistivity (ρ) of as-deposited $(ITO)_{1-x}(ZnO)_x$ film with different x ratio.

x	n	k	N (cm^{-3})	ρ (Ω cm)
0.05	3.22	2.28	3.99×10^{20}	2.52×10^{-2}
0.10	3.33	1.95	4.79×10^{20}	2.12×10^{-2}
0.15	3.76	1.50	8.93×10^{20}	5.4×10^{-3}
0.2	3.65	1.29	8.17×10^{20}	6.16×10^{-3}
0.25	3.62	0.85	7.87×10^{20}	1.45×10^{-2}

where d is the film thickness, T is the transmittance and R is the reflectance.

Using Drude's theory of dielectrics [22], the real dielectric constant (ε') can be written as

$$\varepsilon^{/} = n^2 - k^2 = \varepsilon_i - \frac{e^2}{4\pi^2 c^2 \varepsilon_0}\left(\frac{N}{m^*}\right)\lambda^2, \qquad (3)$$

where ε_i is the infinitely high frequency dielectric constant or the residual dielectric constant due to the ion core, ε_0 is the permittivity of free space, N/m^* is the ratio of carrier concentration to the effective mass, c is the light velocity, λ is the incident light wavelength and e is the elementary charge (1.6×10^{-19} C).

The values of some optical properties of $(ITO)_{1-x}(ZnO)_x$ film with different x ratios in the visible region (320–800 nm) are listed in table 1. The behaviours of free carrier concentration and refractive index are similar. These parameters increase with increasing ZnO ratio up to $x = 0.15$ and then slightly decrease with a further increase in the x ratio, a matter could be correlated to the variation of reflectance with increasing ZnO ratio (figure 4(*b*)). The decrease in extinction coefficient values with increasing x ratio is expected, whereas the transmittance increases with increasing ZnO ratio (figure 4(*a*)). It is also noticed that the electrical resistivity decreases with increasing ZnO ratio to a minimum value of $5.4 \times 10^{-3}\,\Omega$ cm at $x = 0.15$ and then starts to increase, reaching $1.45 \times 10^{-2}\,\Omega$ cm at $x = 0.25$. This behaviour

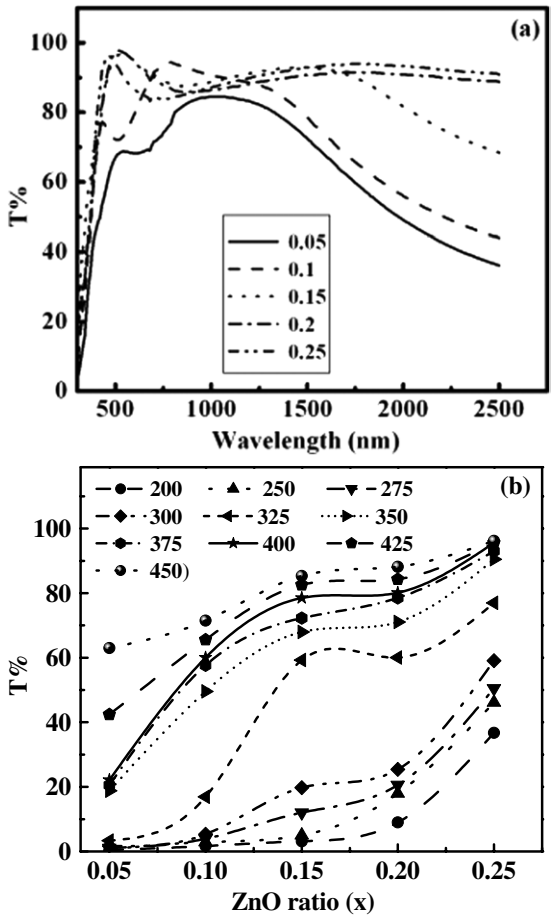

Figure 5. The transmittance spectra of $(ITO)_{1-x}(ZnO)_x$ films with different x ratios annealed at 400 °C (*a*). The average transmittance in the visible region of $(ITO)_{1-x}(ZnO)_x$ films as a function of ZnO ratio at different values of annealing temperature (200–450 °C) (*b*).

of electrical resistivity is due to the behaviour of free carrier concentration listed in table 1.

3.3. The effect of annealing temperature on the optical and electrical properties

Figure 5(*a*) shows the transmission spectra of the considered compositions annealed at 400 °C for 15 min and the dependence of the average value of transmittance in the visible region at different temperatures of annealing (in air) against ZnO ratio (figure 5(*b*)). It is clear that the transmission increases with increasing annealing temperature and ZnO ratio. Besides, at an annealing temperature of 400 °C, the transmittance attains its maximum value 85%, 88% and 96% for $x = 0.15$, 0.2 and 0.25, respectively. The increase in optical transmission with increasing annealing temperature is due to the decrease in oxygen deficiency with annealing in air. Furthermore, the transmittance of $(ITO)_{1-x}(ZnO)_x$ film with $x = 0.05$ seemed to be lower than 64% due to the film opaqueness because the InSn4 peak (1 0 1) still appeared (figure 2(*b*)).

For direct allowed transition, the optical energy gap (E_g) was calculated using equation (4) with the extrapolated

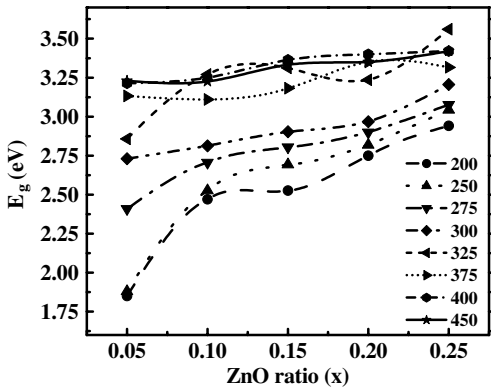

Figure 6. The optical energy gap (eV) versus ZnO ratio for $(ITO)_{1-x}(ZnO)_x$ films at different values of annealing temperature.

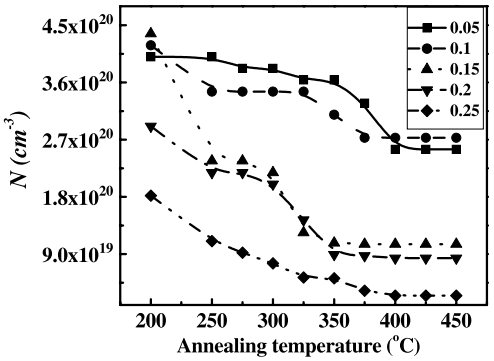

Figure 7. Annealing temperature dependence of free carrier concentration (cm^{-3}) for $(ITO)_{1-x}(ZnO)_x$ films with different ZnO ratios.

intercept of the plot $(\alpha E)^2$ versus the photon energy (E) [23].

$$(\alpha\, E) \propto (E - E_g)^{1/2}. \tag{4}$$

Figure 6 shows the direct optical energy gap as a function of ZnO ratio at different annealing temperatures. The optical band gap increases with increasing zinc oxide ratio and temperature of annealing whereas shifts of the absorption edge to lower values of wavelength have been observed (figure 5(*a*)). Besides, at an annealing temperature of 400 °C for 15 min, the compositions with $x = 0.15$, 0.2, 0.25 have the highest energy gap values of 3.36 eV, 3.4 eV and 3.56 eV, respectively, which are greater than 3.2 eV of ZnO and in the range of (3.5–3.8 eV) for ITO films. This increase in energy gap with annealing temperature may be due to the elimination of the density of localized states between valance and conduction bands. However, its increase with ZnO could be correlated with the increase in the lattice ordering associated with the increase in grain size (figure 3).

The decrease in the value of free carriers concentration from $\sim 10^{20}$ to $\sim 10^{19}$ cm^{-3} with the increase in both annealing temperature and ZnO ratio, as shown in figure 7, can be attributed to the increase in the optical energy gap, which in turn leads to an increase in the optical transmittance.

Plots in figures 8(*a*) and (*b*) indicate that both the refractive index and extinction coefficient decrease with an increase in both ZnO content and annealing temperature. The reduction in the refractive index may be due to the increase in carrier

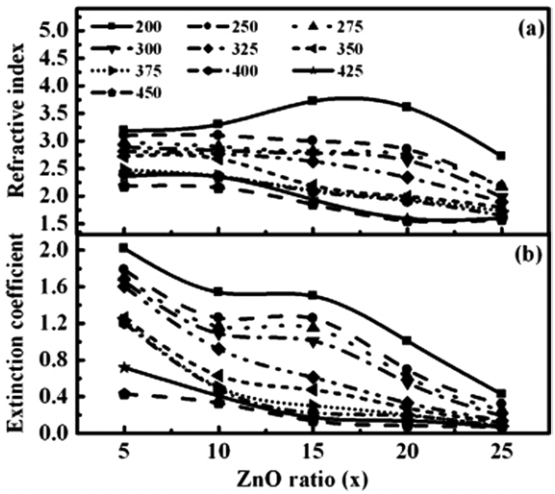

Figure 8. Variations of the average refractive index (*a*) and extinction coefficient (*b*) in the visible region of $(ITO)_{1-x}(ZnO)_x$ films with ZnO ratio at different values of annealing temperature.

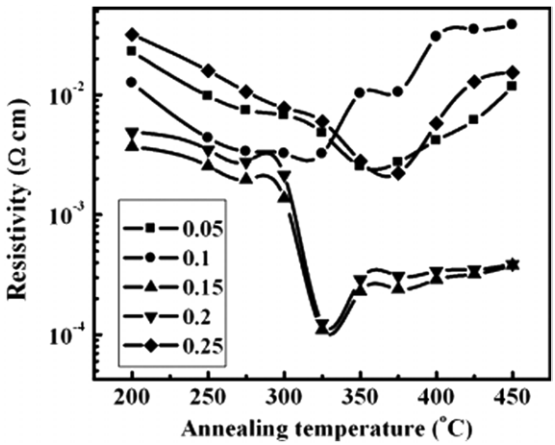

Figure 9. The variation of the electrical resistivity (Ω cm) of $(ITO)_{1-x}(ZnO)_x$ films as a function of annealing temperature for films with different x ratios.

mobility, which leads to an increase in both the relaxation time and the mean free path. On the other hand, according to the relation $k = \alpha\lambda/4\pi$, where λ is the average wavelength in the visible region, the decrease in k with an increase in the annealing temperature is expected, since the absorption coefficient decreases with increasing annealing temperature.

Figure 9 depicts the electrical resistivity of different compositions annealed at different temperatures. The electrical resistivity decreases with elevating annealing temperature up to 325–350 °C and then increases with a further increase in annealing temperature. The minimum values of resistivity are observed for films with $x = 0.15$ and 0.2 which attain their optimum smallest values of 1.1×10^{-4} Ω cm and 1.2×10^{-4} Ω cm, respectively, after annealing temperature at 325 °C for 15 min. Moreover, the mobility of carriers attains its maximum values of 455 $cm^2\ V^{-1}\ s^{-1}$ and 347 $cm^2\ V^{-1}\ s^{-1}$ for films with $x = 0.15$ and 0.2, respectively, annealed at 325 °C as shown in figure 10. The observed improvement in mobility and hence conductivity may be due to the enhancement of the film crystallinity and the grain size growth (figure 3). On the other hand, the high values of resistivity observed after

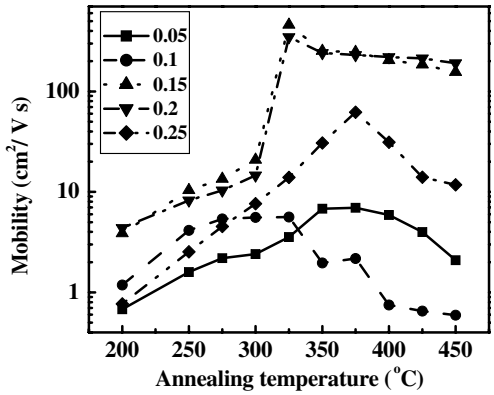

Figure 10. Plot of the calculated carrier mobility ($cm^2\ V^{-1}\ s^{-1}$) against the annealing temperature for $(ITO)_{1-x}(ZnO)_x$ films with different x ratios.

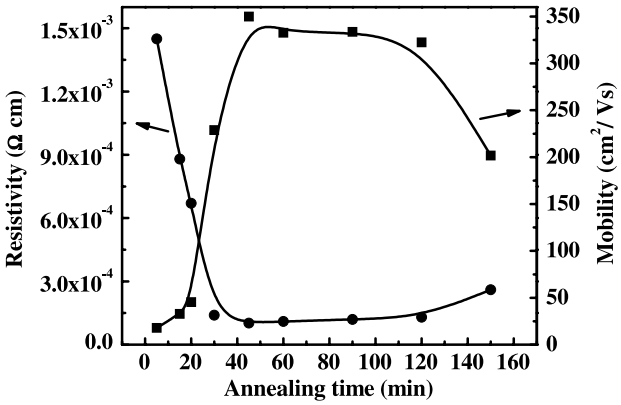

Figure 11. Plot of the measured electrical resistivity (Ω cm) and calculated mobility ($cm^2\ V^{-1}\ s^{-1}$) of $(ITO)_{1-x}(ZnO)_x$ films with $x = 0.2$ annealed at 325 °C for different annealing time.

annealing temperature at 350 °C is due to the chemisorptions process of oxygen taking place on the film surface and in the pores, which acts as an acceptor of electrons from occupied conduction band states [16, 24, 25].

3.4. The effect of annealing time on the optical and electrical properties

Figure 11 depicts the variation of both the electrical resistivity (ρ) and the mobility carriers (μ) of $(ITO)_{1-x}(ZnO)_x$ film with $x = 0.2$ as a function of annealing time at 325 °C. Opposite behaviours of ρ and μ could be observed with annealing time. In fact, one can correlate these behaviours to the increase in the ordering degree of the film with annealing time as previously discussed. For larger times of annealing, the electrical resistivity increases slightly which may be due the increase in the surface roughnes, resulting from the interaction between the glass substrate with the film material at high temperature [26].

Results of the optical parameters, namely, transmittance (T), reflectance (R), optical energy gap (E_g) refractive index (n), extinction coefficient (k) and free carrier concentration (N), are listed in table 2. It is clear that the transmittance reaches its maximum value of 90% after annealing for 120 min. It is seen that the optical energy gap in general increases with

Table 2. The dependence of average Transmittance (T_{vis}), average reflectance (R_{NIR}), optical energy gap (E_g), average refractive index (n_{vis}), average extinction coefficient (k_{vis}) and free carrier concentration (N) on the annealing time at 325 °C for $(ITO)_{1-x}(ZnO)_x$ film with $x = 0.2$.

Annealing time (min)	T% (vis)	R% (NIR)	E_g (eV)	n (vis)	k (vis)	N (10^{20} cm^{-3})
5	15.4	30.9	2.91	3.5	0.578	2.419
15	19.6	28.4	3.0	3.28	0.517	2.161
20	27.3	21.8	3.07	2.75	0.425	2.054
30	29.9	20.3	3.18	2.64	0.401	1.952
45	43.3	19.8	3.19	2.61	0.298	1.819
60	62.7	19.63	3.23	2.59	0.187	1.706
90	83.4	15.57	3.33	2.3	0.102	1.559
120	90.2	9.46	3.35	2.29	0.0802	1.189
150	88	9.45	3.33	2.2	0.084	1.190

prolongation of the annealing period. The maximum optical energy gap value of 3.35 eV was obtained after annealing temperature for 120 min. On the other hand, the behaviours of the other parameters with both annealing time and temperature are generally similar.

Finally, values of 89–90% optical transmittance in visible light and electrical resistivity in the range from 4×10^{-3} to 1.22×10^{-3} Ω cm have been reported [10] as attractive properties of Zn/ITO film as the transparent-conductive one. Also, in reference [16] it was found that low resistivity (2.12×10^{-3}–12×10^{-3} Ω cm) and high visible transmittance of 83% were obtained of zinc oxide doped ITO films. Therefore, the present optimized values 84–90% of transmittance and 1.2×10^{-4}–1.3×10^{-4} Ω cm of electrical resistivity may also be considered as a good result.

3.5. Figure of merit

Figure of merit $\phi = T/\rho$, where T is the average transmittance in the visible region (320–800 nm) and ρ (Ω cm) is the electrical resistivity at room temperature, is a suitable physical terminal used for evaluating the compromise between the electrical and optical properties of a material film and the validity of such material to be promising as a transparent-conductive one. Results of figure of merit are shown in figure 12. It is clear that the film with $x = 0.2$ annealed at 325 °C for 15 min having $T = 72\%$ and $\rho = 1.2 \times 10^{-4}$ Ω cm could be considered as the best transparent-conductive film among the considered films. Moreover, the prolongation of the annealing period was found to improve the film quality, since the figure of merit ϕ significantly increases up to $\sim 69.5 \times 10^4$ $(\Omega\ cm)^{-1}$ after annealing for 90 min. However, for larger times of annealing a slight decrease in the value of ϕ was observed.

4. Summary and conclusions

The present films were elaborated using electron-beam evaporation from a bulky form produced by the sintering process. As-deposited ZnO doped ITO films are partially amorphous, opaque and nonconductive. The heat treatment of films seemed to improve the ordering of the film structure, which in turn significantly enhances the film conduction and mobility. On the other hand, the annealing in air and/or the

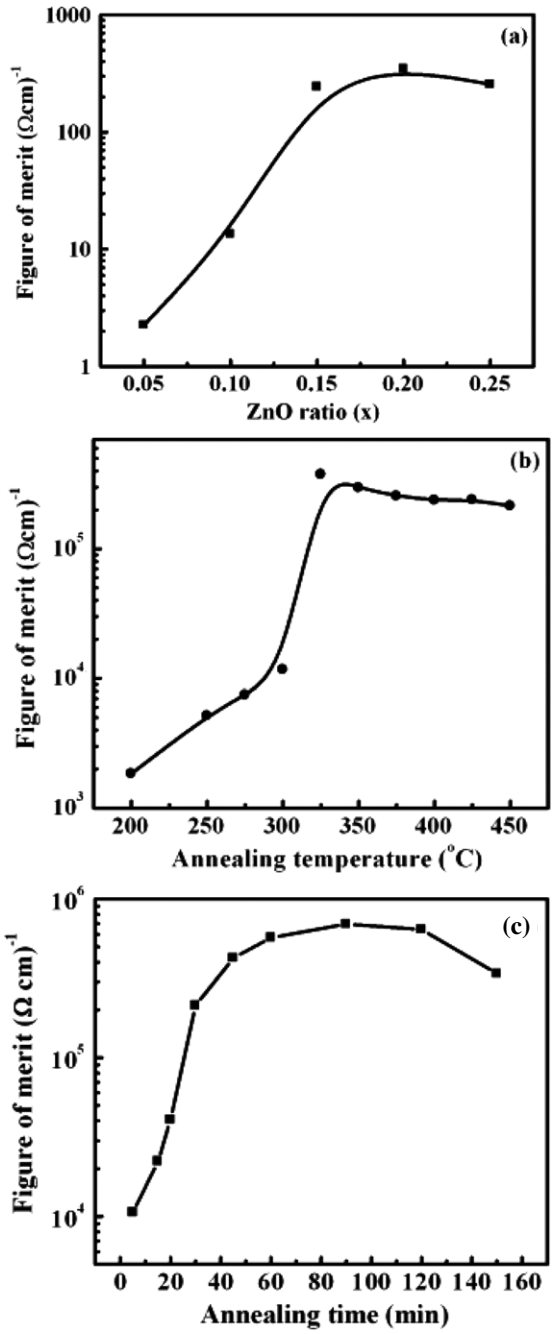

Figure 12. Variations of the figure of merit ϕ for as-deposited $(ITO)_{1-x}(ZnO)_x$ films with ZnO ratio (*a*), at different annealing temperatures for 15 min with $x = 0.2$ (*b*) and at different annealing times at 325 °C (*c*) for $(ITO)_{1-x}(ZnO)_x$ film with $x = 0.2$.

existence of ZnO may substitute some oxygen deficiency in the lattice leading to the increase in the film transmittance. Besides, the parameters, optical energy gap, free carrier concentration, refractive index and extinction coefficient were found to be strongly affected by both heat treatment and ZnO doping.

The satisfactorily optimized low resistivity (1.2×10^{-4}–$1.3 \times 10^{-4}\,\Omega$ cm) and high transmittance in the visible light (84–90%), as well as good adherence to the glass substrate for the present films, may suggest their suitability for many applications in the field of optoelectronic technology.

Acknowledgments

The author would like to thank Professor E Kh Shokr and Dr H M Ali for their continuous encouragement and suggestions during this work.

References

[1] Fahland M, Karlsson P and Charton C 2001 *Thin Solid Films* **392** 334
[2] Tak Y H, Kim K B, Park H G, Lee K H and Lee J R 2002 *Thin Solid Films* **411** 12
[3] Ullal H S, Zweibel K and Von Roedern B 2002 *Proc. 29th IEEE Photovoltaic Specialists Conf. (New Orleans, LA)* p 472
[4] Plá J, Tamasi M, Rizzoli R, Losurdo M, Conturioni E, Summonte C and Rubinell F 2003 *Thin Solid Films* **425** 185
[5] Pankove J I 1980 Display devices *Topics in Applied Physics* vol 40 (Berlin: Springer)
[6] Osaza K, Ye T and Aoyagi Y 1994 *Thin Solid Films* **246** 58
[7] Tanisier L and Garani A 1987 *Electrochim. Acta* **32** 1365
[8] Chopra K L and Das S R 1983 *Thin Films Solar Cell* (New York: Plenum) p 321
[9] Kim H, Gilmore C M, Piqué A, Horwitz J S, Mattoussi H, Murata H, Kafafi Z H and Chrisey D B 1999 *J. Appl. Phys.* **86** 6451
[10] Herrero J and Guillén C 2004 *Thin Solid Films* **451–452** 630
[11] Granqvist C G and Hultaker A 2002 *Thin Solid Films* **411** 1
[12] Jeong S H, Lee S B and Boo J-H 2004 *Curr. Appl. Phys.* **4** 655
[13] Sun X W, Warng L D and Kwok H S 2000 *Thin Solid Films* **360** 75
[14] Minami T, Yamamoto T, Toda Y and Miyata T 2000 *Thin Solid Films* **373** 189
[15] Liu D S, Wu C C and Lee C T 2005 *Japan. J. Appl. Phys.* **44** 5119
[16] Ali H M 2005 *Phys. Status Solidi* a **202** 2742
[17] Kingery W D 1959 *Kinetics of High Temperature Process* ed W Kingery (Cambridge, MA: MIT Press) p 187
[18] Cullity B D 1978 *Elements of X-ray Diffraction* 2nd edn (Reading, MA: Addison Wesley) p 102
[19] Chopra K L, Major S and Pandya D K 1983 Transparent conductors—a status review *Thin Solid Films* **102** 1
[20] Ali H M, Mohamed H A and Mohamed S H 2005 *Eur. Phys. J. Appl. Phys.* **31** 87
[21] Tauc J 1979 *Amorphous and Liquid Semiconductors* ed J Tauc (New York: Plenum) p 159
[22] Weijtens C H L and Van loon P A C 1991 *Thin Solid Films* **196** 1
[23] Ohhata Y, Shinoki F and Yoshida S 1979 *Thin Solid Films* **59** 255
[24] Mohamed S H 2005 *Phys. Status Solidi* a **202** 1948
[25] Choi Y S, Lee C G and Cho S M 1996 *Thin Solid Films* **298** 153
[26] Ramana C V, Smith R J, Hussain O M and Julien C M 2004 *Mater. Sci. Eng.* B **111** 218